Translational Oncology 14 (2021) 100961

Contents lists available at ScienceDirect

Translational Oncology

journal homepage: www.elsevier.com/locate/tranon

Original Research

BEBT-109, a pan-mutant-selective EGFR inhibitor with potent antitumor activity in EGFR-mutant non-small cell lung cancer

Fushun Fan, Minhua Zhou, Xiaolan Ye, Zhenxian Mo, Yaru Ma, Liying Luo, Xiaotong Liang, Haiqi Liu, Yunwo Weng, Mingsheng Lin, Xinjian Liu, Xiong Cai, Changgeng Qian*

Guangzhou BeBetter Medicine Technology Co., Ltd, 25 Yayingshi Road, Guangzhou, 510000, China

ARTICLE INFO

Keywords:
BEBT-109
T790M
exon20ins
G719S
Pan-mutant-selective EGFR inhibitor
NSCLC

ABSTRACT

EGFR mutation-positive NSCLC tumors are highly heterogeneous, therefore, exploring an agent simultaneously targeting multiple EGFR mutations may be valuable for clinical practice. Compared with osimertinib, BEBT-109 shows more sensitive and extensive antitumor activity in EGFR mutant NSCLC, while sparing wild-type EGFR cell lines. Meanwhile, unlike the metabolite of osimertinib AZ5104, the main metabolites of BEBT-109 are found lacking in activity against wild-type EGFR cell lines. Preclinical and clinical studies demonstrate a unique pharmacokinetic profiles of BEBT-109 with rapid absorption and quick *in vivo* clearance without accumulation, which are conducive to minimizing the off-target toxicity of the covalent irreversible EGFR inhibitor. Oral administration of BEBT-109 induces tumor regression in EGFR exon 20 insertion xenografts, and even tumor disappearance in PC-9, HCC827 and H1975 xenograft models. Furthermore, in clinical trials, the objective responses were observed in NSCLC patients with EGFR T790M mutation in the first and second dosing cohorts. These findings demonstrate that BEBT-109, a potent pan-mutant-selective EGFR inhibitor with improved pharmacokinetic properties, might offer a promising new option for the treatment of multiple mutant-EGFR-driven NSCLC.

Introduction

Non-small cell lung cancer (NSCLC) is one of the most prevalent malignant tumors, and the five-year relative survival rate for stage 4 NSCLC is less than 5% after diagnosis [1, 2]. More recently, immune checkpoint inhibitor (ICI) therapy has significantly improved the five-year overall survival rate for patients without driver alterations [3, 4]. However, approximately 10–15% of Caucasian and 30–40% of East Asian NSCLC cases harbor EGFR activating mutations, for whom the treatment outcome of ICI therapy is poor [5–7]. In contrast, EGFR tyrosine kinase inhibitors (EGFR TKIs) have consistently shown superior clinical outcomes and currently represent the best treatment option for this subset of patients.

Exon 19 deletion (Del19) and exon 21 L858R point mutation which are termed as classical mutation approximately account for 45% and 40% of EGFR mutations, respectively [8, 9]. Compared with chemotherapy alone in patients with these common EGFR mutations, the first-generation reversible EGFR TKIs (*i.e.* gefitinib, erlotinib) provide high objective response rate (ORR), prolonged progression-free survival (PFS) and improved quality of life [10–13]. Unfortunately, an acquired resistance usually develops after 10–14 month treatment, caused by a secondary T790M point mutation (the substitution of methionine residue for threonine790) at the gatekeeper position of EGFR in nearly 60% of NSCLC patients who initially respond to the first-generation EGFR-TKI treatment [14, 15]. To overcome the T790M-driven acquired resistance, the second-generation irreversible EGFR TKIs (dacomitinib [16] and afatinib [17]) were developed to potentially provide therapeutic options for T790M positive patients. However, their utilities in the clinical setting are limited by toxicities such as diarrhea and skin rashes resulting from the high wild-type EGFR inhibitory potency [18]. Then, several third-generation irreversible covalent EGFR TKIs (*e.g.*, rociletinib [19], osimertinib [20], olmutinib [21], etc.) have emerged as next-in-line therapeutics to treat EGFR T790M positive tumors. The third-generation EGFR TKIs have a significantly increased selectivity against mutant EGFR and fewer toxicities in comparison with earlier generations. Osimertinib gained accelerated approval by the US FDA in 2015 to treat patients with metastatic EGFR T790M mutation-positive NSCLC whose disease had progressed on or after first-generation EGFR TKI therapy [22]. In April 2018, osimertinib received approval as the first-line treatment of patients with metastatic NSCLC, whose tumors had EGFR Del19 or exon 21 L858R mutation [23]. However, osimertinib is still not free of the typical side effects related to the inhibition of wild-type

* Corresponding author.
E-mail address: cqian@bebettermed.com (C. Qian).

https://doi.org/10.1016/j.tranon.2020.100961
Received 2 October 2020; Received in revised form 11 November 2020; Accepted 13 November 2020

EGFR, which is probably attributed to its pharmacokinetic properties and metabolites, especially AZ5104 [24].

Although excluded from most clinical trials, 10% to 15% of NSCLC tumors harbor uncommon mutations, including point mutations, deletions and insertions within exons 18–25 of the EGFR gene [25]. Among uncommon EGFR mutations in NSCLC, EGFR exon 20 insertion (exon20ins) mutations, accounting for 4–10% of all [26–28], are the third most common type of mutations following L858R and Del19. Exon 20 insertions are highly variable in position and size, which consist of in-frame insertions of 3 to 21 base pairs predominantly within the range from codons 762 to 774 [26]. In contrast to L858R and Del19 mutations, exon 20 insertions are generally associated with resistance to EGFR TKIs. Most NSCLC patients with EGFR exon 20 insertion mutations, except for the rare A763_Y764insFQEA mutation, fail to respond to gefitinib, erlotinib or afatinib, with a reported ORR below 8%, incurring short intervals of disease control in most patients [29–32]. In addition, although some of the ongoing clinical studies have shown preliminary promising activity against exon20ins mutations, there are, however, still no approved molecular targeted drugs for exon20ins NSCLC patients [33–36], which creates an urgent need for the development of more effective therapeutics.

The exon 18 G719X mutations result in substitutions of other residues, primarily alanine (G719A), cysteine (G719C) and serine (G719S), for the glycine at position 719. The G719X mutations representing approximately 3% of all EGFR mutations may occur alone or coexist with EGFR exon 20 S768I (1%) and exon 21 L861Q (1%) mutation [37]. Unlike EGFR exon20ins mutations, G719X substitutions are a mutation of intermediate sensitivity to EGFR TKIs, to which the average response rate of the first-generation inhibitor is 35.1% [38]. In 2018, FDA expanded the frontline indication for afatinib to include NSCLC patients who harbor EGFR alterations in G719X, S768I, L861Q and the complex mutations based on the results of Lux-Lung studies [31].

Recent studies have showed that EGFR mutation-positive non-small-cell lung cancer is highly heterogeneous at the cellular level, and the heterogeneity of EGFR mutations within a single tumor specimen partially leads to the resistance of EGFR-mutant NSCLC to EGFR TKIs [39]. Therefore, exploring an agent simultaneously targeting multiple clinically relevant EGFR mutations may prolong the progression-free survival (PFS) in NSCLC patients. In this study, we report BEBT-109, a novel pan-mutant-selective EGFR inhibitor targeting both TKI-sensitive mutants (Del19, G719A, L861Q and S768I) and TKI-resistant mutants (T790M and exon20ins) with greater *in vitro* potency and *in vivo* antitumor efficacy, less wild-type EGFR activity and fewer off-target toxicities compared with osimertinib. BEBT-109 received investigational new drug (IND) application approval from NMPA in 2019, and is currently in Phase I clinical trials in China.

Materials and methods

Chemicals

Osimertinib, BEBT-109 and its metabolites M5, M6 were synthesized by Guangzhou BeBetter Medicine Technology Co., LTD. The final products were characterized by nuclear magnetic resonance (NMR) and liquid chromatography–mass spectrometry (LC-MS). The purity of these compounds were analyzed by LC-MS methods and showed purity of at least 96%.

Off-target profiling

BEBT-109 (10 μmol/L) was profiled for functional responses against 47 major physiologically important targets by Safety47^{TM} Panel (DiscoverX) following standard manufacturer's procedures ($n = 2$). Those with a percent of response over 75% were further evaluated.

Kinase binding and PathHunter β-arrestin assay

The competition binding assay was performed by KINOMEscan Profiling Service (DiscoverX) [40]. Briefly, DNA-tagged kinases were premixed with immobilized ligand to generate affinity resins for the assay. The percent inhibition of BEBT-109 was negatively correlated with the amount of retained DNA-tag kinase in immobilized ligand which was measured via quantitative PCR of the DNA tag. In this study, binding assays were used for the determination of binding constant (Kd) of BEBT-109 against EGFR, INSR and VEGFR2. BEBT-109 was also tested in antagonist mode with the requested GPCR biosensor assays against CHRM1 and HTR2A [41]. In brief, DiscoverX PathHunter cell lines expressing the tagged-CHRM1 or -HTR2A in tissue culture flasks in the corresponding cell culture medium were dispensed into 384-well microplate. The BEBT-109-treated cells were then measured by PathHunter detection reagent using plate readers. BEBT-109 was handled with an 11-point 3-fold serial dilution starting from the top concentration of 1 or 10 μmol/L in each assay.

Cell culture

Human EGFR mutant NSCLC cell lines (H1975, HCC827 and PC-9) and human EGFR wild-type cells (H460, Calu-6 and LOVO) were obtained from Cell Culture Facility of Chinese Academy of Sciences. IL-3-dependent Ba/F3 cell line was purchased from Guangzhou Cellcook Biotech Co., Ltd.. H1975, HCC827, H460, LOVO and Ba/F3 cells were cultured in RPMI-1640 (GIBCO) supplemented with 10% FBS (Biological Industries) and 1% penicillin-streptomycin (GIBCO). PC-9 cells were grown in Dulbecco's Modified Eagle Medium (GIBCO) supplemented with 10% FBS and 1% penicillin-streptomycin. All cells were maintained and propagated as monolayer cultures at 37 °C in a humidified 5% CO_2 incubator. All human cell lines were routinely authenticated by short-tandem repeat (STR) analysis and verified to be free of mycoplasma contamination.

Constructs and transfections

The indicated site-directed and insertion mutations were constructed by PCR-based methods with the pBABE vector containing full-length wild-type EGFR (Addgene; Plasmid# 20737) as templet. The sequenced EGFR mutants were cloned into the pLEX-MCS lentiviral vector. The virus production, collection and infection were carried out by transfecting the pLEX constructs along with helper plasmids (psPAX2, pMD2.G) into 293T cells following the pLEX-MCS vector manufacturer's instruction. Lentivirus transduced Ba/F3 cells were selected for 1 week with 1 μg/ml puromycin in RPMI-1640 supplemented with 10% FBS and interleukin-3 and then in RPMI-1640 without IL-3 to obtain the EGFR signaling-addicted cells. Lentivirus-transduced H1975 cells were selected for 2 weeks with 2 μg/ml puromycin in RPMI-1640.

Cell proliferation assay

Cells were seeded onto 96-well white microplates (Corning #3610) in their respective growth media at a density of 5000 cells per well and treated with each test compound across an 8-dose range from 0.6 nmol/L to 10 μmol/L on the same day for Ba/F3 cells and the following day for the human NSCLC cells. After treatment with compounds for 72 h, cell viability was measured by the CellTiter-Glo assay (Promega) according to the manufacturer's protocol. The relative cell viability was calculated as a ratio of each value to that of the DMSO control. Experiments were carried out at least twice and cell viability was calculated with GraphPad Prism V5.0 software.

Cell cycle analysis

The H1975 cells (2×10^5 cells/well) were plated into 6-well plates. After adhering to the well, the cells were treated with 1 nmol/L of BEBT-

109 and osimertinib for 24 h and then fixed with 75% ethanol at −20 °C overnight. The fixed cells were washed by PBS and stained with 1 ml DNA staining solution (Multi Sciences, Hang Zhou, China) at room temperature in the dark for 30 min. Stained cells were immediately analyzed by flow cytometer (Millipore, MA, USA) and the data was analyzed with Flowjo software.

Western blotting

Cells were treated with each compound for 6 h and harvested with RIPA buffer supplemented with 1 mmol/L PMSF and protease inhibitor cocktail (Sigma-Aldrich). The lysates were resolved on 8% polyacrylamide gels and transferred to polyvinylidene difluoride membranes (PVDF, immobilon). After blocking in 5% BSA-TBST, membranes were probed with EGFR (BD Biosciences), phosphor-EGFR (Tyr1068, R&D Systems), ERK (Cell Signaling Technology), phospho-ERK (Thr202/Tyr204, Cell Signaling Technology), AKT (Cell Signaling Technology), phospho-AKT (Ser473, Cell Signaling Technology) and anti-GAPDH (Cell Signaling Technology) followed by secondary antibody (IRDye 680 RD Goat anti-Rabbit or IRDye 800 CW Goat anti-Mouse). Signals were detected by ODYSSAY Clx (LAKTI-COR) according to the instrument guidelines.

Metabolite analysis

BEBT-109 (5 μmol/L) was incubated with human liver microsomes (BD gentlest) at 37 °C for 60 min. At different time points (0 min and 60 mins), 135 μl ACN was added to each sample to stop incubation. All samples were vortexed for 20 s and spun at 15,000 rpm for 10 min, and the supernatant was then taken for LC-UV-LTQ analysis. Identification of BEBT-109 metabolite profiles was conducted by Thermo LTQ with ESI (+). The proportion of total area was determined by analyzing the UV traces at 288 nm to assess the relative quantity of BEBT-109 metabolites.

Caco-2 permeability assay

The human colorectal carcinoma cell line caco-2 monolayers in both the apical-to-basolateral (a→b) and the basolateral-to-apical (b→a) directions mimic the permeability of drug across intestinal barrier *in vivo*. The apparent permeability (Papp) values for BEBT-109 and osimertinib were determined in a standardized *in vitro* assay by Shanghai Chempartner Co., Ltd.. Metoprolol, atenolol and erythromycin at the concentration of 10 μmol/L were used as positive control markers for high, low passive permeability and a higher efflux ratio, respectively. Briefly, caco-2 cells forming monolayers on microporous polycarbonate membranes were used in the investigation. The inhibitors to be tested were added to either the apical or the basolateral side of the membrane and the concentrations on the other side were measured by liquid chromatography-tandem mass spectroscopy (LC-MS/MS) after 90 min. Drug permeability was calculated based on the following equation:

$$\mathrm{Papp} = (\mathrm{VA}/(\mathrm{Area} \times \mathrm{time})) \times ([\mathrm{drug}]\mathrm{accepter}/(([\mathrm{drug}]\mathrm{initial,donor}) \times \mathrm{Dilution\ Factor}),$$

Where VA is the volume in the acceptor well, area is the surface area of the membrane and time is the total transport time in seconds.

In vivo *pharmacokinetics/pharmacodynamics studies*

7- or 8-week-old H1975 tumor-bearing specific-pathogen-free (SPF) BALB/c nude mice from Beijing Vital River Laboratory Animal Technology Co., Ltd. were randomly divided into different groups (3 mice/group) when the tumor volumes reached 260–865 mm^3 for oral (60 mg/kg) administration. Temporal-concentration curve was measured from the collected analytical data of the concentrations of BEBT-109 in plasma, tumor tissues and brain tissues 0.5, 1, 2, 4, 8 and 24 h after drug administration by LC-MS/MS assay. PKSolver (version 2.0) was used to analyze the pharmacokinetic parameters. The tumor tissues were cut into two parts for assaying EGFR L858R T790M phosphorylation by immunoblotting analysis.

For mouse models of brain metastasis, approximately 3×10^5 H1975 cells were implanted into the brains of immunodeficient BALB/c nude mice purchased from Beijing Vital River Lab. The microsyringe was used for microliter injection. As the tumors grew, six tumor-bearing mice were randomly divided into two groups ($n = 3$/group), and the plasma, brain tumor and tumor-free tissue were harvested one or two hours after an oral dose of BEBT-109 at 60 mg/kg. The samples were then placed in liquid nitrogen, and transferred to the −80 °C refrigerator before LC-MS/MS determination.

Immunohistochemistry

The tumor tissues were fixed in 4% formalin for 24 h at room temperature, then dehydrated and embedded in paraffin. The 4-μm-thick sections were deparaffinized, rehydrated and covered with primary Ki67 (Proteintech Inc) and phosphor-EGFR (Cell Signaling Technologies) antibody at 4 °C overnight. Then, the samples were incubated with HRP-conjugated secondary antibody for one hour and DAB staining for detection. Finally, the positively stained cells were evaluated by digital image analysis with Image J software.

Xenograft studies

All mouse studies were performed in compliance with the agreement of the Institutional Animal Care and Use Committee of Guangzhou BeBetter Medicine Technology Co., Ltd. guidelines. Approximately 2–5×10^6 cells/ml cells were subcutaneously inoculated into the right armpits of 7- to 8-week-old female BALB/c nude mouse (Beijing Vital River Laboratory Animal Technology Co., Ltd. or Guangdong Medical Lab Animal Center) in a total volume of 0.1 ml PBS/mouse for tumor development. In particular, PC-9 cells were suspended within 50% matrigel (Biocoat). Mice were randomly assigned to the different treatment groups ($n = 8$/group). When the tumor volumes reached around 200–300 mm^3, the mice were treated with the test compounds. Tumor size were measured by a bilateral caliper, and the tumor volumes were calculated with the formula $V = (\mathrm{length} \times \mathrm{width}^2)/2$.

Clinical study

The clinical study was a Phase I, multicenter, single-arm, open-label, dose-escalation study that determined the safety, tolerability, pharmacokinetics (PK), and efficacy of BEBT-109 in locally advanced or metastatic non-small cell lung cancer patients with EGFR T790M mutation after treatment with at least one EGFR-TKI. Before enrolling in a clinical trial, all patients should provide written informed consent and the clinical study (CTR20192575) was approved by appropriate institutional review boards at each participating sites (for the 2 patients disclosed in this article, the trial protocol is reviewed by Ethics Committee of Hunan Cancer Hospital and The Affiliated Cancer Hospital of Xiangya School of Medicine). 6 dose cohorts were designed for the first-in-human dose escalation study. In order to enroll as many as patients to a dose that may be clinically beneficial, if no drug-related grade 2 non-hematological toxicity or grade 3 hematological toxicity were observed, only one patient is included in the starting and second dose group. Efficacy was assessed by RECIST 1.1. Blood samples were collected on Day 1 and Day 28 at 0 (before dosing), 1, 1.5, 2, 3, 5, 8, 12, and 24 h after treatment of BEBT-109 to obtain pharmacokinetic data.

Statistical analysis

Data are represented as average ± SEM. Comparisons between two groups were conducted by use of two-tailed student's t-test. Statistical significance of multiple comparisons was determined by two-way ANOVA (tumor volume) and long-rank tests (survival curve) with a P value less than 0.05.

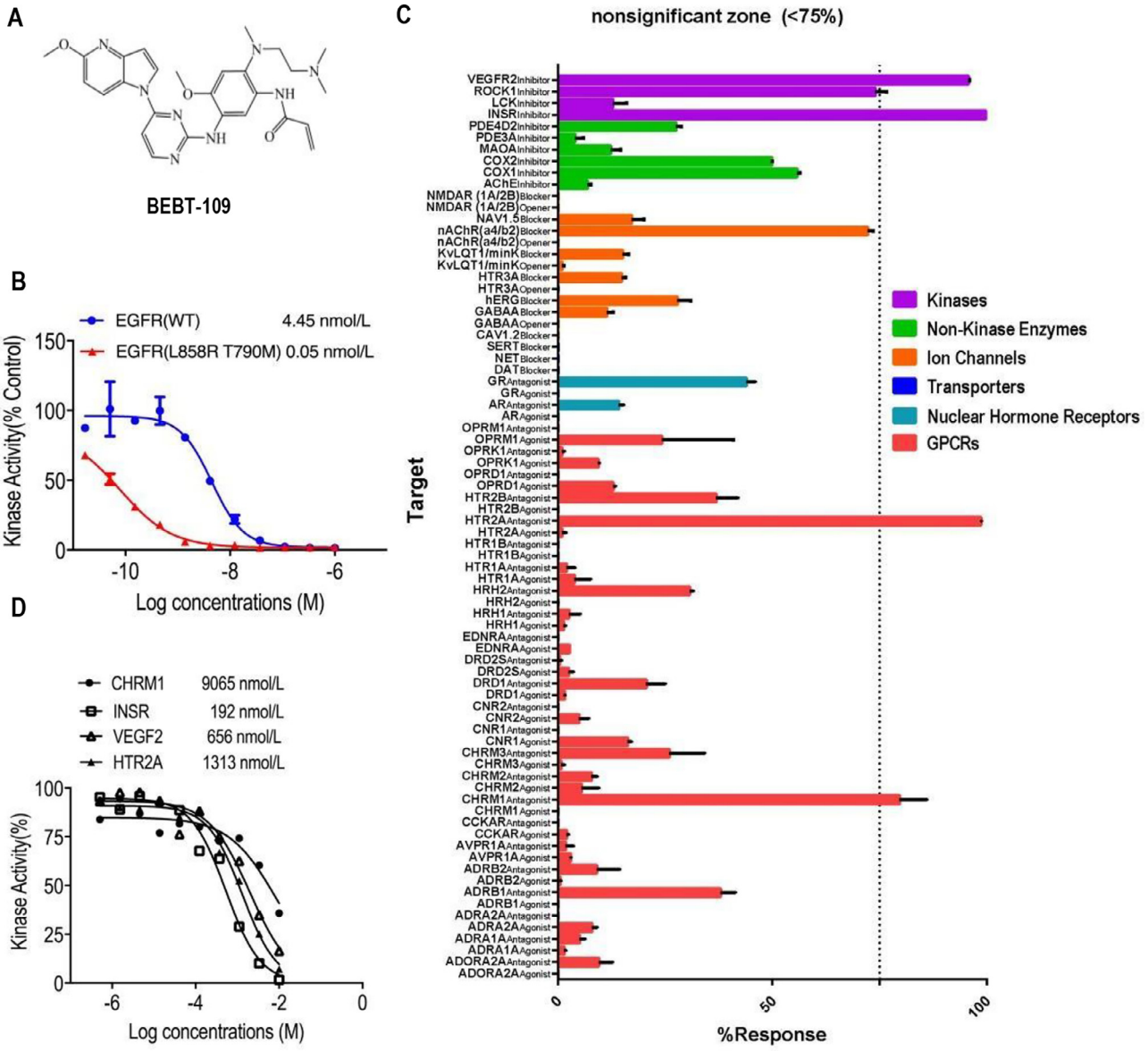

Fig. 1. BEBT-109 structure and its selectivity profile. **A,** Chemical structure of BEBT-109. **B,** EGFR binding assay was performed to determine the selectivity and potency of BEBT-109 ($n = 2$). **C,** *In vitro* pharmacologic profiling assay was used to assess the potential off-target effects of BEBT-109 (10 μmol/L) against major targets. Graph represents mean percent response+SEM. Values less than 75% (indicated by dashed lines) were considered nonsignificant zone ($n = 2$). **D,** Kinase affinities of BEBT-109 against CHRM1, INSR, VEGFR2 and HTR2A were determined by kinase binding and PathHunter β-arrestin assay ($n = 2$).

Results

BEBT-109 is a mutant-specific EGFR tyrosine kinase inhibitor

We designed and discovered a novel class of irreversible inhibitors of EGFR tyrosine kinase mutants with an acrylamide moiety that irreversibly binds to the EGFR kinase domain by targeting the Cys797 residue in the ATP binding pocket. Among these compounds, BEBT-109 is one extremely potent and mutant-specific EGFR inhibitor (Fig. 1A). To determine its selectivity and potency, EGFR binding assay was performed by use of recombinant wild-type EGFR and mutant EGFR L858R T790M kinases. BEBT-109 showed an apparent binding affinity with a binding constant (Kd) of 0.05 nmol/L against EGFR L858R T790M, which was nearly 90 times more potent than its binding to wild-type EGFR with a Kd of 4.45 nmol/L (Fig. 1B).

To investigate the undesirable off-target activity of BEBT-109, its ability to interact with a variety of proteins were evaluated *in vitro* by use of commercial Safety47 Panel (DiscoverX). BEBT-109 showed minimal potential off-target effects in only 4 of 78 assays at a dose of 10 µmol/L, namely insulin receptor (INSR), muscarinic acetylcholine receptor M1 (CHRM1), 5-hydroxytryptamine receptor 2A (HTR2A) and vascular endothelial growth Factor 2 (VEGFR2) (Fig. 1C). The kinase activities of BEBT-109 against these four proteins were further determined. The IC_{50} or Kd values of CHRM1, HTR2A, INSR, and VEGFR2 were 9065 nmol/L, 1313 nmol/L, 192 nmol/L, and 656 nmol/L, respectively (Fig. 1D), which were much higher than that of EGFR L858R T790M (Fig. 1B). These results indicated low off-target, apparent specificity of BEBT-109 against mutant EGFR, suggesting a safety index suitable for further development.

BEBT-109 selectively suppresses EGFR TKI-sensitive mutants in vitro

To evaluate the cellular potency of BEBT-109, we compared it with osimertinib in cell viability and EGFR phosphorylation assays

by use of a number of human NSCLC cell lines or murine Ba/F3 cells ectopic expressing EGFR G719A, L861Q and S719I mutants. It was found that BEBT-109 showed stronger anti-proliferation activity against EGFR TKI-sensitive mutant cell lines, including PC-9 (Del19), HCC827 (Del19), Ba/F3-EGFR-G719A, Ba/F3-EGFR-L861Q and Ba/F3-EGFR-S768I with mean IC_{50} values ranging from 1.7 to 51.7 nmol/L (Fig. 2A, B and E). In particular, the potencies against the G719A and L861Q mutants were 11.7 folds and 5.6 folds higher than those of osimertinib, respectively (Fig. 2B and E). In the meantime, BEBT-109 and osimertinib have very weak potency against EGFR wild-type cell lines (H460, Calu-6 and LOVO) and EGFR-deficient Ba/F3 cells, with mean IC_{50} values over 1000 nmol/L (Fig. 2C-E).

The efficacy of BEBT-109 against the phosphorylation of EGFR was further examined by immunoblot analysis of lysates from PC-9 cells bearing Del19 mutation and Ba/F3 cells ectopic expressing EGFR G719A mutants. As shown in Fig. 2F, both BEBT-109 and osimertinib inhibited the phosphorylation of EGFR and its downstream signaling substrates (phospho-AKT and phospho-ERK) in a dose-dependent manner. In line with the cell viability data, BEBT-109 more potently inhibited phosphor-EGFR than osimertinib. Collectively, those data suggested that BEBT-109 had better potency and selectivity than osimertinib in growth inhibition of tumor cells harboring EGFR TKI-sensitive mutants (Del19, G719A, L861Q and S768I).

BEBT-109 selectively inhibits EGFR TKI-resistant mutants in vitro

Since the T790M secondary mutation has emerged as a cause for treatment failure in NSCLC patients who initially respond to first-generation EGFR TKIs, we next evaluated the potency of BEBT-109 against the acquired T790M resistance with H1975 cell. The CellTiter-Glo assay showed that BEBT-109 was more effective against EGFR L858R T790M mutation compared with osimertinib (Fig. 3A and C), with mean IC_{50} values of 1.0 nmol/L and 3.9 nmol/L for BEBT-109 and osimertinib, respectively.

Furthermore, we evaluated the efficacy of BEBT-109 against EGFR exon 20 insertions, which are generally associated with resistance to current EGFR TKIs. The full-length EGFR with the top five prevalent forms of exon 20 insertion (A763_Y764insFQEA, A767_V769dupASV, D770_N771insSVD, N771_H773dup and P772_H773dup) [36] was individually introduced into H1975 and Ba/F3 cell lines, which were used to evaluate the anti-proliferation role of BEBT-109. The average IC_{50} values were found ranging from 7.8 nmol/L to 73.1 nmol/L in exon20ins-expressing H1975 cells and from 10.5 nmol/L to 32.1 nmol/L in exon20ins-expressing Ba/F3 cells, respectively, which were approximately 4 to 5 folds more sensitive than osimertinib (Fig. 3B and C, Supplementary Fig. S1A and B). The efficacy of BEBT-109 in suppressing cell growth was further validated by crystal violet staining (Fig. 3D). We next examined the effect of BEBT-109 on cell-cycle progression in H1975 cells. 1 nmol/L BEBT-109 induced accumulation of cells in the G0/G1 phase, however, 1 nmol/L osimertinib did not change the cell cycle profile (Fig. 3E).

The differences in efficacy between BEBT-109 and osimertinib in cell growth against T790M mutation and EGFR exon 20 insertion mutations were reproduced in western blotting experiments in H1975 cell line and EGFR A767_V769dupASV mutant expressing H1975 and Ba/F3 cells. It was found that BEBT-109 more effectively suppressed EGFR and its downstream signaling pathway phosphorylation in a dose-dependent manner and caused considerable inhibition at 10 nmol/L, making BEBT-109 approximately 10 times more potent than osimertinib (Fig. 3F and G). So far, our experiments have demonstrated a profound anti-proliferation efficacy of BEBT-109 against both EGFR TKI-sensitive mutants and TKI-resistant mutants *in vitro*.

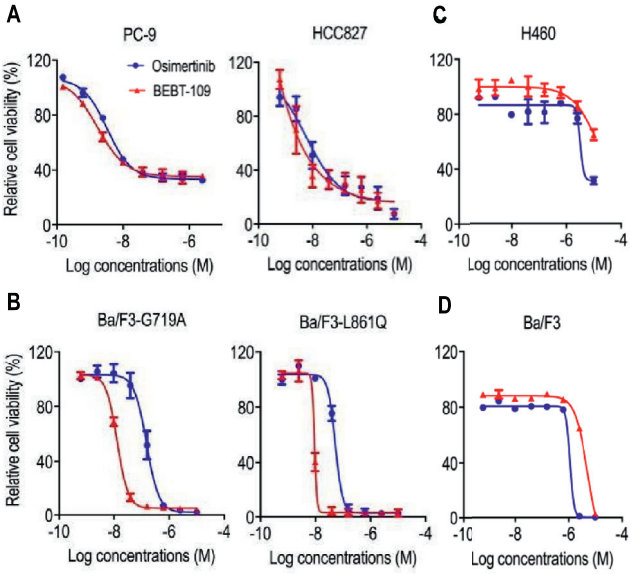

E

EGFR status	Cell line	IC_{50} (nmol/L)	
		BEBT-109	Osimertinib
Del19	PC-9	4.8	9.8
Del19	HCC827	1.7	3.3
G719A	Ba/F3	13.0	151.8
L861Q	Ba/F3	9.3	52.2
S768I	Ba/F3	51.7	198
WT	H460	>10000	3162
	Calu-6	>10000	4317
	LOVO	1304	1283
-	Ba/F3(IL-3+)	3415	1112

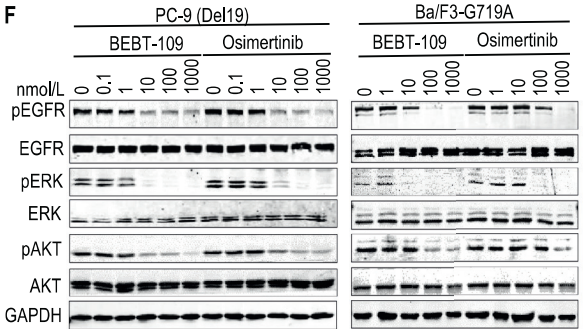

Fig. 2. BEBT-109 selectively suppresses EGFR TKI-sensitive mutants *in vitro*. **A-D,** In comparison with osimertinib, BEBT-109 exhibited greater potency in reducing the viability of cells harboring TKI-sensitive mutants(Del19, G719A and L861Q) (**A and B**) ($n = 3$), while having less activity against EGFR wild-type H460 cells and EGFR-deficiency Ba/F3 cells (**C and D**) ($n = 2$), as assessed by use of CellTiter-GLO assay after 3 days of treatment. **E,** IC_{50} values of BEBT-109 and osimertinib for EGFR wild-type cells ($n = 2$), EGFR-deficient Ba/F3 cells ($n = 2$) and mutant EGFR-expressing cells ($n = 3$). **F,** PC-9 cells (Del19) and Ba/F3 cells expressing EGFR G719A were treated with the indicated concentrations of BEBT-109 and osimertinib for 6 h. Phosphorylation of EGFR and its downstream signaling substrates were evaluated by western blotting with the indicated antibodies.

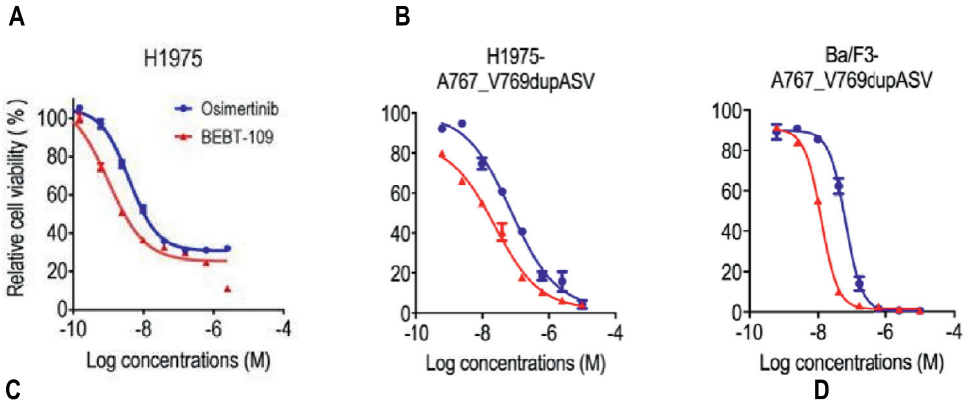

C

EGFR Status	H1975 IC_{50} (nmol/L)		Ba/F3 IC_{50} (nmol/L)	
	BEBT-109	Osimertinib	BEBT-109	Osimertinib
A763_Y764insFQEA	7.8	24.6	10.5	44.8
A767_V769dupASV	34.4	154.4	20.8	101.1
D770_N771insSVD	73.1	305.2	32.1	110.3
N771_H773dup	70.0	274.9	20.7	88.5
P772_H773dup	56.0	214.8	15.3	58.9
Parent	1.0	3.9	3415	1112

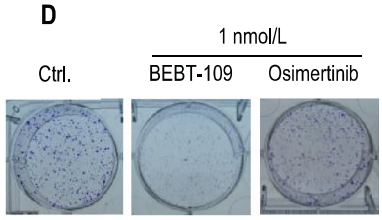

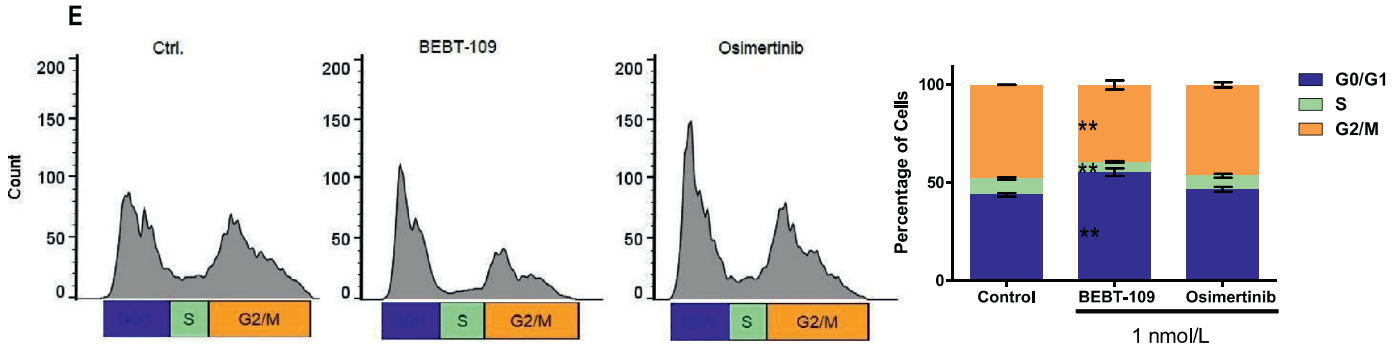

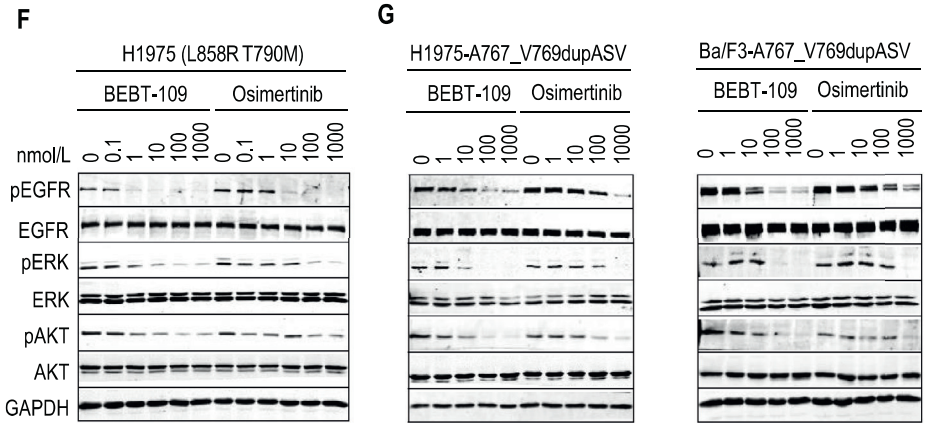

Fig. 3. Inhibition of cell growth and EGFR phosphorylation in cells expressing EGFR TKI-resistant mutants by BEBT-109. **A and B,** H1975 (L858R T790M) **(A)** and exon20ins-expressing H1975 and exon20ins-expressing Ba/F3 cells **(B)** were treated with serially diluted BEBT-109 and osimertinib for 72 h. Cell viability was measured using the CellTiter-Glo assay ($n=3$). **C,** IC_{50} values of BEBT-109 and osimertinib against various exon20ins mutations of H1975 and Ba/F3 cells, and EGFR-deficient Ba/F3 cells ($n=3$). **D,** A total of 1000 H1975 cells were treated with DMSO, 1 nmol/L BEBT-109 or 1 nmol/L osimertinib for 1 weeks. The plates were stained with crystal violet and visually examined. **E,** BEBT-109 causes G1 arrest at 1 nmol/L. H1975 cells were exposed to 1 nmol/L BEBT-109 and osimertinib for 24 h ($n=3$), $^{**}p<0.01$ vs control group. **F and G,** Inhibition of EGFR phosphorylation and its downstream signaling pathway in H1975 cells **(F)** and H1975 and Ba/F3 cells with ectopic expressing EGFR-A767_V769dupASV **(G)** treated with BEBT-109 or osimertinib for 6 h was evaluated using western blotting.

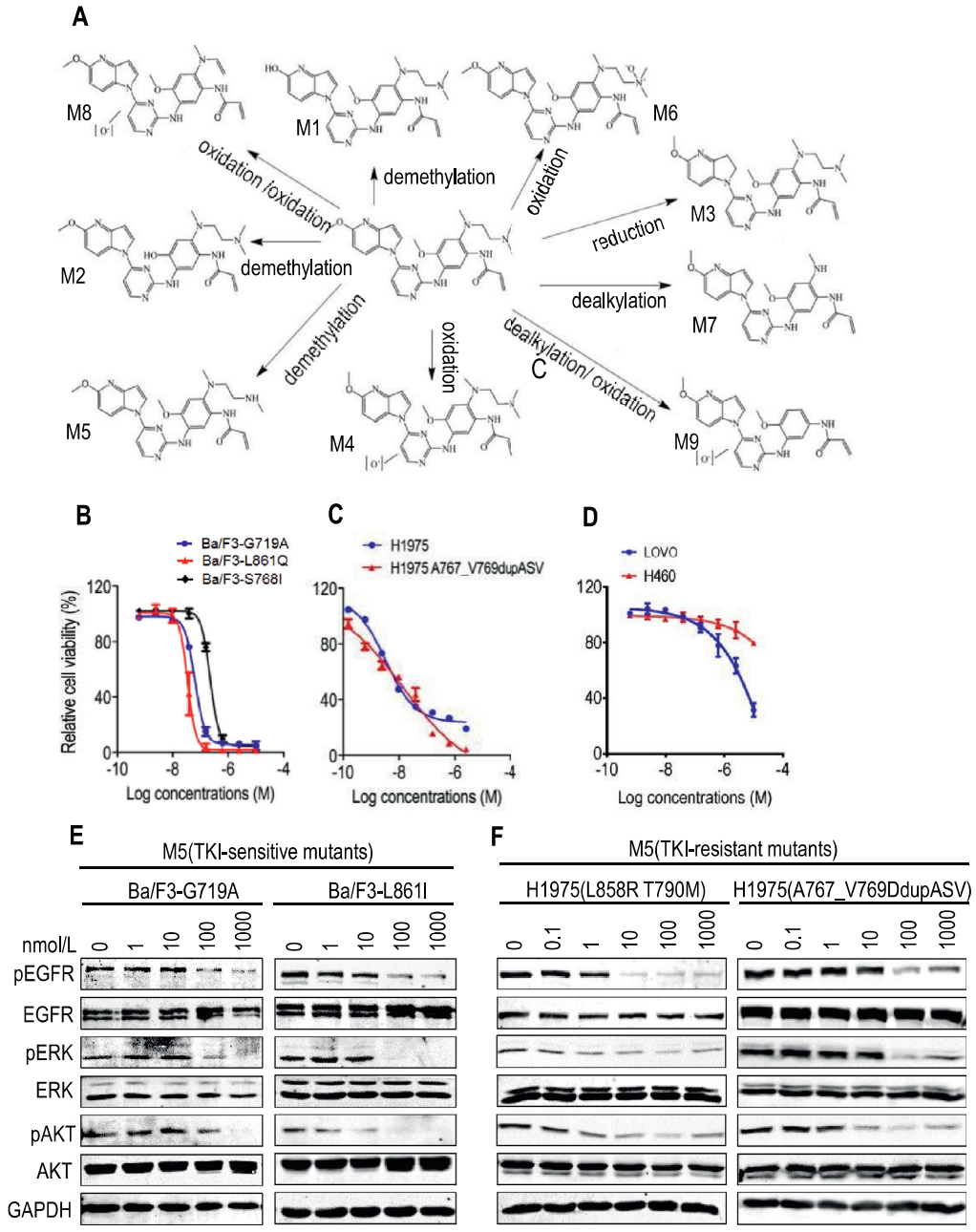

Fig. 4. Metabolite of BEBT-109 (M5) inhibits cell growths and EGFR phosphorylation against EGFR-mutant NSCLC. **A,** Proposed BEBT-109 metabolic pathways show the formation of metabolites (M1-M9). **B-D,** Cell growth inhibition of BEBT-109 metabolic substance M5 in cell lines expressing EGFR TKI-sensitive mutants ($n = 3$) **(B)**, EGFR TKI-resistant mutants ($n = 3$) **(C)** and wild type EGFR ($n = 2$) **(D). E and F,** Effects of EGFR phosphorylation and its downstream signaling pathways by BEBT-109 metabolic substances (M5) in cells expressing EGFR TKI-sensitive **(E)** and TKI-resistant **(F)** mutants.

Metabolites of BEBT-109 show potent anti-proliferation activity and no off-target effects

BEBT-109 was incubated with mouse and human liver microsomes to identify its metabolites by LC-UV combined LTQ linear ion trap mass spectrometer analysis. Nine metabolites (M1-M9, Supplementary Fig. S2A) were identified as products presumptively through oxidation, demethylation, reduction or dealkylation pathways (Fig. 4A). BEBT-109 displayed a similar panel of metabolites across species, and M5 (demethylation) and M6 (oxidation) are two dominant ones (Supplementary Fig. S2A-B).

M5 and/or M6 metabolites exhibited high potency against cell lines with EGFR TKI-sensitive mutations (Del19, G719A, L861Q and S768I) and TKI-resistant mutations (T790M and exon 20 insertion mutations), while having much less activity *versus* EGFR wild-type or EGFR-deficient (Ba/F3) cell line (Fig. 4B-D, Supplementary Fig. S2C and D). In line with the cell viability data, M5 metabolites showed a dose-dependent inhibition of EGFR and its downstream signaling substrates phosphorylation against TKI-sensitive mutant- and TKI-resistant mutant-expressing cell lines *in vitro* (Fig. 4E and F).

Pharmacokinetic and pharmacodynamic properties of BEBT-109

To evaluate pharmacokinetic (PK) and pharmacodynamic (PD) properties of BEBT-109, we first carried out a caco-2 permeability assay to predict human oral absorption of BEBT-109. In this assay, BEBT-109

A

	Papp (×10⁶/cm·s⁻¹) A→B	B→A	Papp(B-A) /Papp(A-B)
BEBT-109	11.35	8.66	0.76
Osimertinib	1.32	2.11	1.59

B

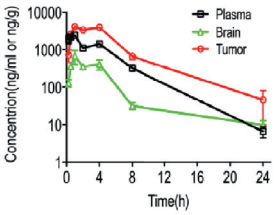

C

Parameter	Plasma	Tumor	Brain
$t_{1/2}$(h)	2.65	3.44	3.88
T_{max}(h)	1	1	1
C_{max}(ng/ml or ng/g)	2420	4120	682
AUC_{0-24}(ng/ml/h or ng/g/h)	12370	28270	2838

D

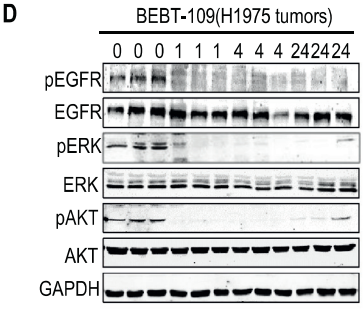

G

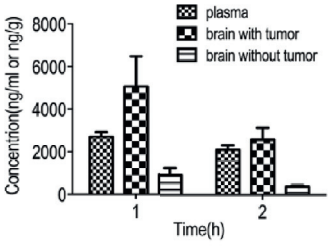

E

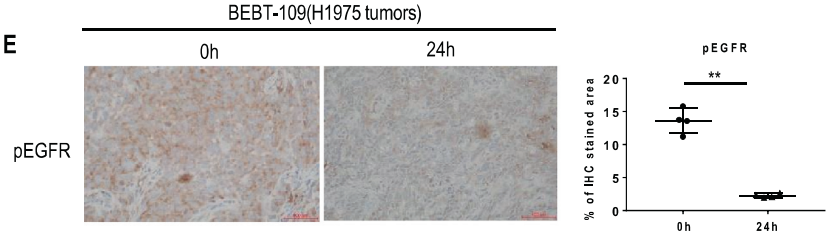

F

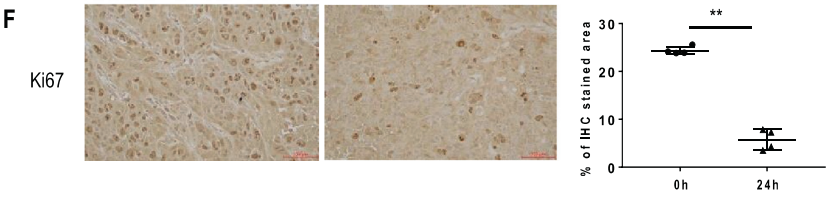

Fig. 5. Pharmacokinetic and pharmacodynamic properties of BEBT-109. **A,** Permeability of BEBT-109 and osimertinib across caco-2 cell monolayers ($n = 2$). **B and C,** BEBT-109 pharmacokinetics in plasma, tumor and brain in H1975 xenograft model following oral administration of BEBT-109 at 60 mg/kg ($n = 3$). **D,** Western blot analysis of EGFR and its downstream signaling substrates phosphorylation in three tumor samples obtained from tumor-bearing nude mice treated with 60 mg/kg BEBT-109 orally. **E and F,** Immunohistochemistry staining of phosphor-EGFR (E) and Ki67 (F) in control H1975 tumors (0 h) and BEBT-109-treated tumors (24 h) ($n = 4$). $^{**}p<0.01$ vs control group. Scale bars = 100 μm. **G,** Distribution to mouse brain tumor of BEBT-109 in H1975 cell xenograft intracranial transplantation mice ($n = 3$).

showed an apparent permeability 7.6 folds higher than osimertinib and the efflux of BEBT-109 was also relatively lower, indicating a favorable oral absorption in human (Fig. 5A).

After oral dosing of BEBT-109 at 60 mg/kg in H1975 xenograft mouse model, the plasma, brain and tumor tissues were harvested in various time points. LC-MS/MS assay revealed that the time of maximum concentration observed (T_{max}) and the half-life ($T_{1/2}$) of BEBT-109 were around 1.0 hour and 3.44 h in tumor after oral administration, respectively. The AUC and the maximum concentration observed (C_{max}) of BEBT-109 in tumors were 28,270 ng/g•h, and 4120 ng/g, respectively (Fig. 5B and C). The pharmacokinetic studies indicated a rapid absorption, a high C_{max} and moderate clearance properties of BEBT-109 in tumor tissues. Furthermore, western blot analysis demonstrated that the phosphorylation of EGFR and its downstream signaling substrates in tumors was almost totally abolished 1 hour after BEBT-109 treatment (Fig. 5D). Although the $T_{1/2}$ of BEBT-109 was approximately 3.44 h in tumors (Fig. 5C), phosphor-EGFR signal remained to be completely blocked even 24 h after treatment (Fig. 5D), which indicates BEBT-109 exhibits persistent target inhibition after the drug clearance. IHC analysis further confirmed that phosphor-EGFR expression and the number of proliferating cells also significantly decreased in the BEBT-109-treated mice compared with that in the vehicle-treated mice for 24 h after treatment (Fig. 5E and F).

Micromolar concentrations were detected in brain tissues after oral dose, which indicated BEBT-109 could cross the blood-brain barrier (Fig. 5B and C). To mimic brain metastasis of lung cancers, we then carried out experiments in the human H1975 intracranial brain tumor mice model. The concentrations of BEBT-109 in brain tumors, tumor-free brains and plasma were measured 1 hour (T_{max}) and 2 h after oral administration of BEBT-109 at 60 mg/kg. As shown in Fig. 5G, the mean concentrations of BEBT-109 in plasma, tumor-free brains and brain tumors 1 hour after administration were 2696.7 ng/ ml, 927.0 ng/g and 5061.7 ng/g, respectively. The ratios of brain tumors/plasma and brain tumors/tumor-free brains were 1.23 times and 5.46 times, respectively. Similar data were acquired from samples two hours after BEBT-109 treatment. The distribution of BEBT-109 of higher concentration in brain

tumors suggested that BEBT-109 would be beneficial to treat primary and metastatic brain tumors with EGFR mutation.

BEBT-109 selectively inhibits mutant NSCLC in vivo

To investigate the *in vivo* antitumor efficacy of BEBT-109, various mutant EGFR xenograft models representing clinical NSCLC setting were generated in nude mice. In H1975 (L858R T790M) tumor xenograft model, once the tumor volume reached about 200 mm^3, the mice were treated with BEBT-109 (7.5, 15, 30 and 60 mg/kg), osimertinib (25 mg/kg) or vehicle daily for four consecutive weeks. Once-daily dosing of BEBT-109 induced dose-dependent growth inhibition with good tolerance indicated by the modest body weight loss (Fig. 6A, Supplementary Fig. S3A). Similar to the treatment of osimertinib at the maximum tolerated doses (MTD) of 25 mg/kg, 30 and 60 mg/kg, BEBT-109 administration induced complete H1975 tumor regression that allowed host mice survival beyond 30 days post treatment (Fig. 6A and B). At an MTD dose, both BEBT-109 (60 mg/kg) and osimertinib (25 mg/kg) in mice bearing HCC827 (Del19) or PC-9 (Del19) xenografts induced complete tumor regression (Fig. 6C and E) and host mice survival (Fig. 6D and F).

For the EGFR exon 20 insertion mutation model, the mice with EGFR A767_V769dupASV expressing H1975 xenograft tumors were treated with BEBT-109 (10, 20, and 40 mg/kg, bid), osimertinib (20 mg/kg, qd, which was MTD in this model) or vehicle daily for 12 days. The treatment with BEBT-109 induced significant dose-dependent tumor growth inhibition in H1975 EGFR-A767_V769dupASV xenografts (Fig. 6G). With the dose of MTD (40 mg/kg, bid), BEBT-109 treatment showed better antitumor efficacy than osimertinib(20 mg/kg, qd). We further confirmed the antitumor efficacy of BEBT-109 against exon 20 insertion mutations by use of the EGFR A767_V769dupASV-driven Ba/F3 tumor model. Oral administration of BEBT-109 at an MTD dose of 40 mg/kg (bid) for 14 days led to statistically significant inhibition of tumor growth. However, sustained tumor regression was not observed after osimertinib treatment at an MTD dose (Fig. 6H). Neither drug caused significant body weight loss (Supplementary Fig. S3B-E). These experiments therefore indicated that BEBT-109 has a profound growth-suppressive effect against tumors harboring EGFR TKI-sensitive and TKI-resistant mutations.

BEBT-109 demonstrates potent antitumor activity in EGFR T790M-mutant NSCLC patients

BEBT-109 is currently in a Phase I clinical trial (CTR20192575) in locally advanced or metastatic non-small cell lung cancer patients with EGFR T790M mutation after treatment with at least one EGFR-TKI. Here, we describes preliminary clinical activity results for two patients who received BEBT-109 in the first and second cohorts. The first patient harbors the R831H/L858R/T790M EGFR mutation after showing disease progression upon treatment with icotinib or pemetrexed and carboplatin. Administration of BEBT-109 led to tumor shrinkage of 33.7% at the lowest dose(20 mg/day) for 17 weeks(Fig. 7A). The second patient with EGFR Del19 T790M mutant lung adenocarcinoma had progressed following 11-month treatment of AZD3759. Once-daily dosing of BEBT-109 at 40 mg/kg exhibited a tumor reduction of 50.3% after 14-week treatment(Fig. 7B). Preliminary clinical pharmacokinetic profile from the patient in the 20 mg/kg group at day 1 and day 28 indicates BEBT-109 is rapidly absorbed and has quick *in vivo* clearance without accumulation (Fig. 7C).

Discussion

Precision medicine is evolving rapidly and achieving breakthroughs with the occurrence and application of new mutational detection techniques such as next-generation sequencing (NGS) technologies, which have revolutionized the treatment of EGFR mutation-positive NSCLC. Many patients with EGFR mutation-positive NSCLC have been significantly benefited from the availability of several EGFR-targeted agents. Most of the current EGFR-targeted TKIs approved by FDA mainly target Del19 and L858R mutations or an acquired T790M mutation. However, a wider implementation of NGS for diagnostic purposes has demonstrated that EGFR uncommon mutations are more prevalent than previously thought [42]. Meanwhile, given the intratumoral EGFR mutational heterogeneity, genetic alterations co-occur at a high frequency in EGFR mutation-positive NSCLC. Therefore, ideal TKIs should have a broad inhibitory profile to mitigate the heterogeneity of tumors and the risk of rapid expansion of resistant subclones [39].

The efficacy osimertinib in a first-line setting excelled over standard-first line treatment in patients with EGFR-mutant NSCLC regardless of T790M mutation status [43–45]. Although recent research has also revealed that osimertinib shows some benefits for patients with EGFR exon 20 insertion, G719X and L861Q mutations [36, 46], its clinical activities against these mutants still can't meet clinical needs due to its relatively poor targeted activity. In this paper, we discovered a compound that has excellect activities in multiple EGFR mutants while sparing wide-type EGFR. As shown in Fig. 6I, BEBT-109 showed potent inhibitory effects against EGFR TKI-sensitive mutants (Del19, L858R, G719A, L861Q and S768I) and TKI-resistant mutants (T790M and exon20ins). In particular, the anti-proliferation activities of BEBT-109 against G719A, L861Q, T790M and exon20ins mutations are 11.7 times, 5.6 times, 3.9 times and 4.1 times higher than those of osimertinib, respectively, which makes it potentially a promising candidate for a pan-mutant-selective EGFR inhibitor.

It has been reported that AZ5104, an active metabolite of osimertinib, showed great potency against Del19 (2 nmol/L in PC-9) and T790M (2 nmol/L in H1975), and had low selectivity in wild-type EGFR (33 nmol/L in LOVO) cell lines [20]. Two major metabolites of BEBT-109 (M5 and M6) exhibited high potency in a number of EGFR-mutant cell lines, while having weak activity toward EGFR wild-type (LOVO) or EGFR-deficiency (Ba/F3) cell lines. These data suggest that BEBT-109 has higher metabolic tolerability than osimertinib against wild-type EGFR cells, which potentially provides a wider therapeutic index in the clinical application.

For covalent binding irreversible drugs, the prolonged duration of drug action on the target uncouples the pharmacodynamics from the pharmacokinetics of exposure, as target inhibition persists after the drug has been cleared. Therefore, a covalent drug is preferably cleared rapidly to minimize off-target interactions, which could conceivably reduce non-mechanism-based off-target toxicities [47–49]. In view of this, in order to minimize the off-target toxicity of the covalent EGFR inhibitor, BEBT-109 was designed to have more rapid absorption (short T_{max} and high C_{max}) and quicker *in vivo* clearance (short $T_{1/2}$) without accumulation (reduced AUC).

In *in vitro* caco-2 assay, BEBT-109 showed a relatively lower efflux and an apparent permeability 7.6 folds higher than osimertinib, which may allow a more rapid (T_{max}) and higher absorption (C_{max}) of this compound after oral dosing in human.

According to the results from the PK/PD study in the H1975 xenograft model and the preliminary clinical pharmacokinetic analysis, BEBT-109 had moderate clearance after oral dosing. However, the inhibition of EGFR and its downstream oncoprotein (AKT and ERK) phosphorylation in the tumors remained blocked even 24 h after BEBT-109 treatment. Our data suggest, as EGFR covalent irreversible inhibitor, the prolonged duration of BEBT-109 action on the target uncouples the pharmacodynamics from the pharmacokinetics of exposure, but may abate wild-type EGFR inhibition of exposure and off-target toxicities.

In addition to demonstrating potent antitumor efficacy in preclinical mouse xenograft models, the confirmed response described in this article showed proof-of-principle clinical activity in a patient with T790M acquired resistance. Because the plasma concentration of BEBT-109 at the lowest dose was within the effective range, it is possible that BEBT-109 will achieve a good clinical response in the higher-dose group. Mean-

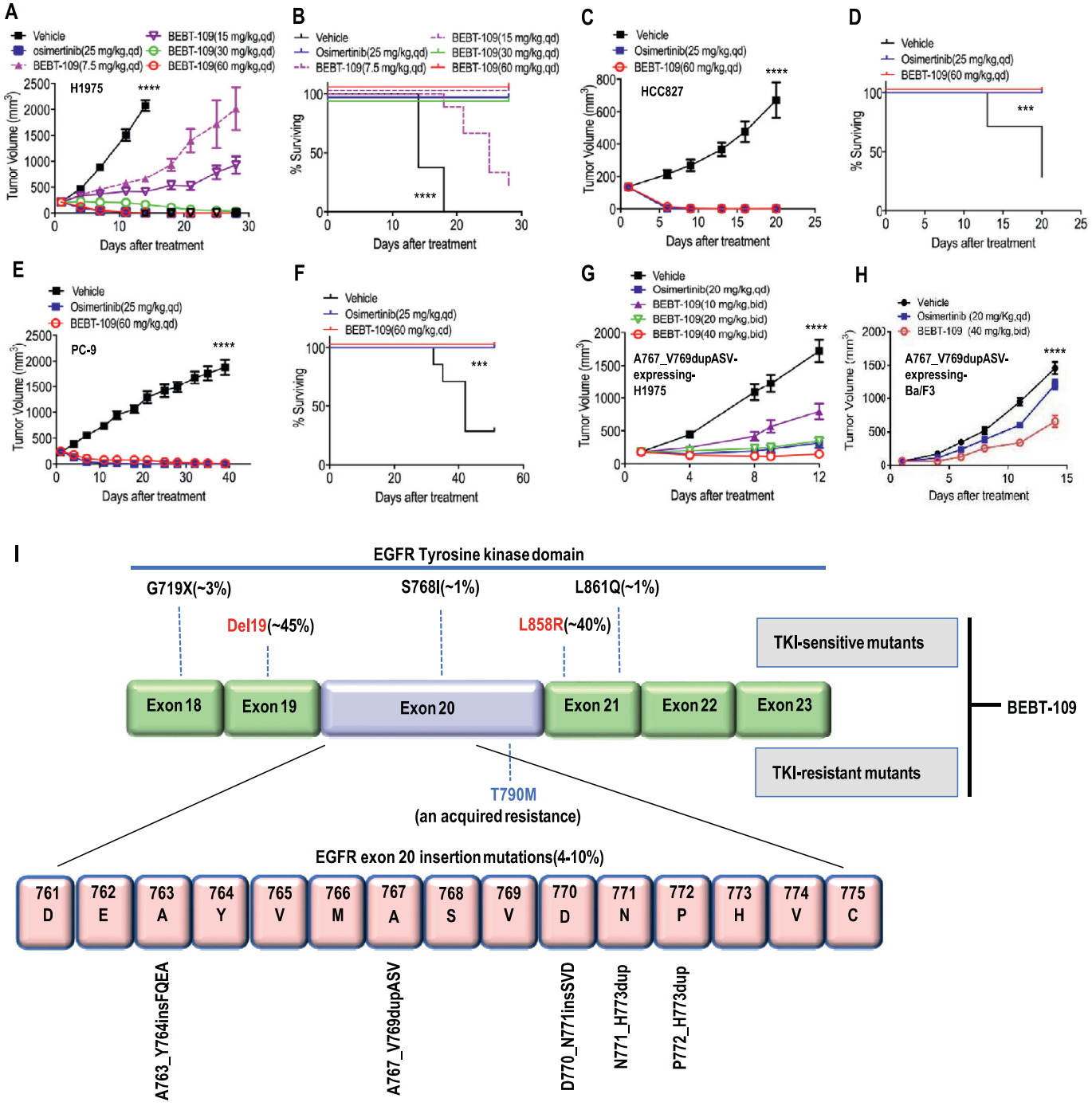

Fig. 6. *In vivo* antitumor efficacy of BEBT-109 in subcutaneous xenograft models of EGFR mutant lung cancer. **A and B,** H1975 (L858R T790M) xenografts following 28-day treatment ($n = 8$) of osimertinib (25 mg/kg) and various doses of BEBT-109. 30 mg/kg and 60 mg/kg BEBT-109 showed the same tumor growth inhibition ability (**A**) and host mice survival (**B**) as 25 mg/kg osimertinib. **C-F,** HCC827 (Del19) and PC-9 (Del19) xenografts following 20- or 40-day treatments ($n = 8$) at 25 mg/kg osimertinib and 60 mg/kg BEBT-109, respectively. BEBT-109 showed the same tumor growth inhibition ability **(C, E)** and host mice survival **(D, F)** as osimertinib. **G,** H1975 (L858R T790M) with EGFR-A767_V769dupASV xenografts following 12 days of daily treatment ($n = 8$) osimertinib and various doses of BEBT-109. BEBT-109 (40 mg/kg bid) showed more potent activity of tumor growth inhibition compared with osimertinib (20 mg/kg qd, MTD in this model). **H,** EGFR-A767_V769dupASV-driven Ba/F3 xenografts following 14 days of daily treatment ($n = 8$) osimertinib and BEBT-109. BEBT-109 (40 mg/kg bid) showed better tumor growth inhibition ability than that of osimertinib (20 mg/kg qd). Data in **A, C,** and **E** represent mean tumor volume ± SEM. $^{****}p<0.0001$, $n = 8$, Two-way ANOVA for A on day 14, C and E; $^{***}p<0.001$, $^{****}p<0.0001$, $n = 8$, Log-rank test for **B, D** and **F. I,** EGFR mutations within exon 18–23 of the tyrosine kinase domain of the gene. Common, uncommon and an acquired resistance EGFR mutations are represented by red, black and blue font respectively. BEBT-109 shows potent inhibitory effect against EGFR TKI-sensitive mutants (Del19, G719A, L861Q and S768I) and TKI-resistant mutants (T790M and exon20ins).

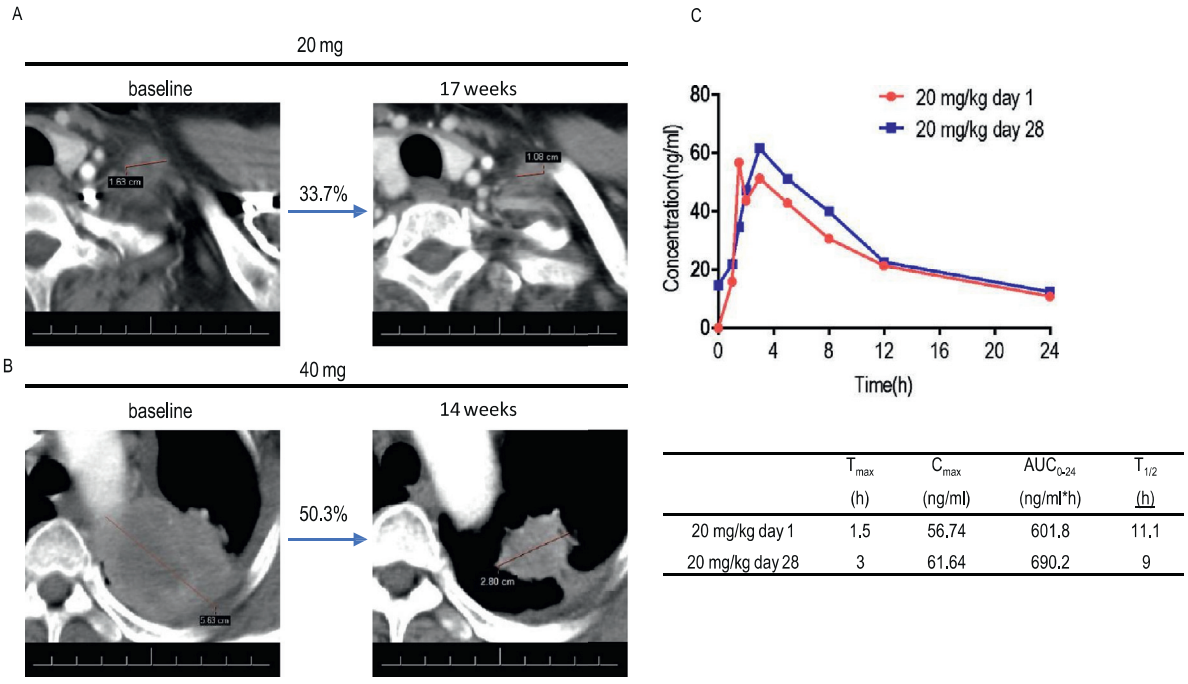

	T_{max} (h)	C_{max} (ng/ml)	AUC_{0-24} (ng/ml*h)	$T_{1/2}$ (h)
20 mg/kg day 1	1.5	56.74	601.8	11.1
20 mg/kg day 28	3	61.64	690.2	9

Fig. 7. Tumor response assessments and preliminary pharmacokinetic profile of BEBT-109 in patients with NSCLC harboring EGFR T790M mutation in a first-in-human dose-escalation study. **A**, Computed tomographic scan images of metastatic region in left supraclavicular lymph nodes from patient with NSCLC harboring EGFR L858R T790M R831H mutation before and after BEBT-109 treatment in phase I clinical trial. The patient was previously treated with Icotinib and followed by 6 cycles of pemetrexed plus carboplatin. Patient was administered BEBT-109 at a dose of 20 mg once per day, and tumor shrinkage of 33.7% was observed. Lesions are outlined by a red line. **B**, Computed tomographic scan images of left upper lobe from patient with NSCLC harboring EGFR Del19 T790M mutation before and after BEBT-109 treatment in phase I clinical trial. The patient was previously treated with AZD3759. Patient was administered BEBT-109 40 mg/kg/day, and tumor shrinkage of 50.3% was observed. Lesions are denoted by a red line. **C**, Preliminary pharmacokinetic profiles from the patient in the 20 mg/day group at day 1 and day 28.

while, we plan to perform a Phase 2 study of BEBT-109 in NSCLC patients with exon 20 insertion and other rare mutations in EGFR.

In summary, our novel compound BEBT-109, a potent pan-mutant-selective EGFR inhibitor, optimized with fewer wide-type EGFR activities from its metabolites and fewer off-target toxicities by improving pharmacokinetic properties of covalent irreversible inhibitors might demonstrate unique therapeutic properties in clinical trials and offer new options for the treatment of multiple EGFR-mutant-driven NSCLC.

Declaration of Competing Interest

The authors are employees of Guangzhou BeBetter Medicine Technology Co., Ltd. C.Q. and X.C. have ownership interest (including patents) in the company.

CRediT authorship contribution statement

Fushun Fan: Methodology, Validation, Formal analysis, Investigation, Data curation, Writing - original draft, Writing - review & editing, Visualization, Supervision. **Minhua Zhou:** Methodology, Validation, Formal analysis, Investigation. **Xiaolan Ye:** Methodology, Validation, Formal analysis, Investigation. **Zhenxian Mo:** Investigation, Visualization. **Yaru Ma:** Investigation, Visualization. **Liying Luo:** Investigation. **Xiaotong Liang:** Investigation. **Haiqi Liu:** Investigation, Visualization. **Yunwo Weng:** Resources. **Mingsheng Lin:** Resources. **Xinjian Liu:** Methodology, Visualization, Writing - review & editing, Visualization. **Xiong Cai:** Conceptualization, Writing - review & editing, Supervision. **Changgeng Qian:** Conceptualization, Writing - review & editing, Supervision, Project administration, Funding acquisition.

Acknowledgments

The work is partly supported by Grant 2014ZT05Y232 from the Department of Science and Technology of Guangdong Province, China and grant 201909020004 from Guangzhou Municipal Science and Technology Bureau. Our appreciation also goes to Professor Chuanyuan Li for his helpful discussion and review of the manuscript.

Supplementary materials

Supplementary material associated with this article can be found, in the online version, at doi:10.1016/j.tranon.2020.100961.

References

[1] R.S. Herbst, J.V. Heymach, S.M. Lippman, Lung cancer, N. Engl. J. Med. 359 (13) (2008) 1367–1380.
[2] F. Bray, et al., Global cancer statistics 2018: GLOBOCAN estimates of incidence and mortality worldwide for 36 cancers in 185 countries, CA Cancer J. Clin. 68 (6) (2018) 394–424.
[3] K.C. Arbour, G.J. Riely, Systemic therapy for locally advanced and metastatic non-small cell lung cancer: a review, JAMA 322 (8) (2019) 764–774.
[4] N.A. Rizvi, et al., Activity and safety of nivolumab, an anti-PD-1 immune checkpoint inhibitor, for patients with advanced, refractory squamous non-small-cell lung cancer (CheckMate 063): a phase 2, single-arm trial, Lancet Oncol. 16 (3) (2015) 257–265.
[5] J.F. Gainor, et al., EGFR mutations and ALK rearrangements are associated with low response rates to PD-1 pathway blockade in non-small cell lung cancer: a retrospective analysis, Clin. Cancer Res. 22 (18) (2016) 4585–4593.
[6] C.K. Lee, et al., Checkpoint inhibitors in metastatic EGFR-mutated non-small cell lung cancer-a meta-analysis, J. Thorac. Oncol. 12 (2) (2017) 403–407.
[7] R.S. Herbst, et al., Pembrolizumab *versus* docetaxel for previously treated, PD-L1-positive, advanced non-small-cell lung cancer (KEYNOTE-010): a randomised controlled trial, Lancet 387 (10027) (2016) 1540–1550.
[8] A. Kumar, et al., Structure and clinical relevance of the epidermal growth factor receptor in human cancer, J. Clin. Oncol. 26 (10) (2008) 1742–1751.

[9] T.J. Lynch, et al., Activating mutations in the epidermal growth factor receptor underlying responsiveness of non-small-cell lung cancer to gefitinib, N. Engl. J. Med. 350 (21) (2004) 2129–2139.
[10] V.D. Cataldo, et al., Treatment of non-small-cell lung cancer with erlotinib or gefitinib, N. Engl. J. Med. 364 (10) (2011) 947–955.
[11] T. Kato, et al., Afatinib *versus* cisplatin plus pemetrexed in Japanese patients with advanced non-small cell lung cancer harboring activating EGFR mutations: subgroup analysis of LUX-Lung 3, Cancer Sci. 106 (9) (2015) 1202–1211.
[12] T.S. Mok, et al., Gefitinib or carboplatin-paclitaxel in pulmonary adenocarcinoma, N. Engl. J. Med. 361 (10) (2009) 947–957.
[13] R. Rosell, et al., Erlotinib *versus* standard chemotherapy as first-line treatment for European patients with advanced EGFR mutation-positive non-small-cell lung cancer (EURTAC): a multicentre, open-label, randomised phase 3 trial, Lancet Oncol. 13 (3) (2012) 239–246.
[14] L.V. Sequist, et al., Genotypic and histological evolution of lung cancers acquiring resistance to EGFR inhibitors, Sci. Transl. Med. 3 (75) (2011) p. 75-26.
[15] W. Pao, et al., Acquired resistance of lung adenocarcinomas to gefitinib or erlotinib is associated with a second mutation in the EGFR kinase domain, PLoS Med. 2 (3) (2005) e73.
[16] J.A. Engelman, et al., PF00299804, an irreversible pan-ERBB inhibitor, is effective in lung cancer models with EGFR and ERBB2 mutations that are resistant to gefitinib, Cancer Res. 67 (24) (2007) 11924–11932.
[17] D. Li, et al., BIBW2992, an irreversible EGFR/HER2 inhibitor highly effective in preclinical lung cancer models, Oncogene 27 (34) (2008) 4702–4711.
[18] N. Katakami, et al., LUX-Lung 4: a phase II trial of afatinib in patients with advanced non-small-cell lung cancer who progressed during prior treatment with erlotinib, gefitinib, or both, J. Clin. Oncol. 31 (27) (2013) 3335–3341.
[19] A.O. Walter, et al., Discovery of a mutant-selective covalent inhibitor of EGFR that overcomes T790M-mediated resistance in NSCLC, Cancer Discov. 3 (12) (2013) 1404–1415.
[20] D.A. Cross, et al., AZD9291, an irreversible EGFR TKI, overcomes T790M-mediated resistance to EGFR inhibitors in lung cancer, Cancer Discov. 4 (9) (2014) 1046–1061.
[21] E.S. Kim, Olmutinib: first Global Approval, Drugs 76 (11) (2016) 1153–1157.
[22] S. Khozin, et al., Osimertinib for the treatment of metastatic EGFR T790M mutation–positive non-small cell lung cancer, Clin. Cancer Res. 23 (9) (2017) 2131–2135.
[23] S.S. Ramalingam, et al., Osimertinib as first-line treatment of EGFR mutation-positive advanced non-small-cell lung cancer, J. Clin. Oncol. 36 (9) (2018) 841–849.
[24] M.R. Finlay, et al., Discovery of a potent and selective EGFR inhibitor (AZD9291) of both sensitizing and T790M resistance mutations that spares the wild type form of the receptor, J. Med. Chem. 57 (20) (2014) 8249–8267.
[25] P.T. Harrison, S. Vyse, P.H. Huang, Rare epidermal growth factor receptor (EGFR) mutations in non-small cell lung cancer, Semin. Cancer Biol. 61 (2020) 167–179.
[26] M.E. Arcila, et al., EGFR exon 20 insertion mutations in lung adenocarcinomas: prevalence, molecular heterogeneity, and clinicopathologic characteristics, Mol. Cancer Ther. 12 (2) (2013) 220–229.
[27] M. Beau-Faller, et al., Rare EGFR exon 18 and exon 20 mutations in non-small-cell lung cancer on 10 117 patients: a multicentre observational study by the French ERMETIC-IFCT network, Ann. Oncol. 25 (1) (2014) 126–131.
[28] M.E. Arcila, et al., Prevalence, clinicopathologic associations, and molecular spectrum of ERBB2 (HER2) tyrosine kinase mutations in lung adenocarcinomas, Clin. Cancer Res. 18 (18) (2012) 4910–4918.
[29] H. Yasuda, S. Kobayashi, D.B. Costa, EGFR exon 20 insertion mutations in non-small-cell lung cancer: preclinical data and clinical implications, Lancet Oncol. 13 (1) (2012) e23–e31.
[30] J. Naidoo, et al., Epidermal growth factor receptor exon 20 insertions in advanced lung adenocarcinomas: clinical outcomes and response to erlotinib, Cancer 121 (18) (2015) 3212–3220.
[31] J.C. Yang, et al., Clinical activity of afatinib in patients with advanced non-small-cell lung cancer harbouring uncommon EGFR mutations: a combined post-hoc analysis of LUX-Lung 2, LUX-Lung 3, and LUX-Lung 6, Lancet Oncol. 16 (7) (2015) 830–838.
[32] G.R. Oxnard, et al., Natural history and molecular characteristics of lung cancers harboring EGFR exon 20 insertions, J. Thorac. Oncol. 8 (2) (2013) 179–184.
[33] J.P. Robichaux, et al., Mechanisms and clinical activity of an EGFR and HER2 exon 20-selective kinase inhibitor in non-small cell lung cancer, Nat. Med. 24 (5) (2018) 638–646.
[34] Z. Yang, et al., A phase 2 study of poziotinib in patients with EGFR or HER2 exon 20 mutation-positive non-small cell lung cancer, J. Clin. Oncol. 36 (15_suppl) (2018) TPS9106 -TPS9106.
[35] R.C. Doebele, et al., First report of safety, PK, and preliminary antitumor activity of the oral EGFR/HER2 exon 20 inhibitor TAK-788 (AP32788) in non–small cell lung cancer (NSCLC), J. Clin. Oncol. 36 (15_suppl) (2018) 9015 -9015.
[36] W. Fang, et al., EGFR exon 20 insertion mutations and response to osimertinib in non-small-cell lung cancer, BMC Cancer 19 (1) (2019) 595.
[37] S. Watanabe, et al., Effectiveness of gefitinib against non-small-cell lung cancer with the uncommon EGFR mutations G719X and L861Q, J. Thorac. Oncol. 9 (2) (2014) 189–194.
[38] K. Li, et al., Determining EGFR-TKI sensitivity of G719X and other uncommon EGFR mutations in non-small cell lung cancer: perplexity and solution (Review), Oncol. Rep. 37 (3) (2017) 1347–1358.
[39] S. Kohsaka, et al., Tumor clonality and resistance mechanisms in EGFR mutation–positive non-small-cell lung cancer: implications for therapeutic sequencing, Future Oncol. 15 (6) (2019) 637–652.
[40] M.A. Fabian, et al., A small molecule-kinase interaction map for clinical kinase inhibitors, Nat. Biotechnol. 23 (3) (2005) 329–336.
[41] X. Zhao, et al., A homogeneous enzyme fragment complementation-based beta-arrestin translocation assay for high-throughput screening of G-protein-coupled receptors, J. Biomol. Screen 13 (8) (2008) 737–747.
[42] K. Y, M. T, Not all epidermal growth factor receptor mutations in lung cancer are created equal: perspectives for individualized treatment strategy, Cancer Sci. 107 (9) (2016) 1179–1186.
[43] P.A. Janne, et al., AZD9291 in EGFR inhibitor-resistant non-small-cell lung cancer, N. Engl. J. Med. 372 (18) (2015) 1689–1699.
[44] T.S. Mok, et al., Osimertinib or platinum-pemetrexed in EGFR T790M-positive lung cancer, N. Engl. J. Med. 376 (7) (2017) 629–640.
[45] S.L. Greig, Osimertinib: first global approval, Drugs 76 (2) (2016) 263–273.
[46] J.H. Cho, et al., Osimertinib for patients with non-small-cell lung cancer harboring uncommon EGFR mutations: a multicenter, open-label, phase II trial (KCSG-LU15-09), J. Clin. Oncol. 38 (5) (2020) 488–495.
[47] J. Singh, et al., The resurgence of covalent drugs, Nat. Rev. Drug Discov. 10 (4) (2011) 307–317.
[48] R. Mah, J.R. Thomas, C.M. Shafer, Drug discovery considerations in the development of covalent inhibitors, Bioorg. Med. Chem. Lett. 24 (1) (2014) 33–39.
[49] V. Pilla Reddy, et al., Development, verification, and prediction of osimertinib drug–drug interactions using PBPK modeling approach to inform drug label, CPT Pharmacometr. Syst. Pharmacol. 7 (5) (2018) 321–330.